Plasmonics
https://doi.org/10.1007/s11468-025-03083-4

RESEARCH

Green One-Pot Synthesis of Silver and Gold Nanoparticles Using Catechin Extracts: Influence of Temperature and Antioxidant Activity Evaluation

Gönül Serdar[1] · Gülşah Gül Kılınç[2] · Tugba Mazlum Şen[3]

Received: 9 April 2025 / Accepted: 28 May 2025

Abstract
In this study, gold (Au) and silver (Ag) nanoparticles were synthesized from an aqueous solution of catechin extract obtained by sequential microwave extraction (MAE) and supercritical fluid extraction (SFE) for the first time at different temperatures (25, 35, 45 °C) in accordance with the characteristics of green chemistry. For the synthesis of Ag and Au nanoparticles at three different temperatures, 100 mL of an aqueous 1 mM $AgNO_3$ solution was added to different volumes (0.5–4 mL) of catechin extract solutions. In the biosynthesis of Ag and Au nanoparticles, 1 mM $AgNO_3$ solution and 0.5 mM $HAuCl_4.3H_2O$ at 25 °C and 0.5 mL extract volume were determined as the best parameters. The crystalline structures of AgNP and AuNP nanoparticles synthesized using catechin extract in accordance with green chemistry principles were confirmed by X-ray diffraction (XRD) analysis. The average crystallite sizes were determined to be 18.82 nm for AgNPs and 14.31 nm for AuNPs. Transmission electron microscopy (TEM) revealed size distributions of 19.50 ± 5.52 nm for AgNPs and 20.06 ± 5.38 nm for AuNPs. Dynamic light scattering (DLS) analysis showed that the hydrodynamic diameters were 37.61 ± 1.25 nm for AgNPs and 37.9 ± 0.26 nm for AuNPs. The zeta potential values were measured as –20.4 mV for AgNPs and –22.6 mV for AuNPs. The PDI (polydispersity index) values were found to be 0.271 ± 0.006 for AgNPs and 0.295 ± 0.004 for AuNPs. The effects of various concentrations of AgNPs and AuNPs on DPPH (2,2-diphenyl-1-picrylhydrazyl) radical scavenging activity were determined. At a concentration of 0.91 mg/mL, AgNPs exhibited a high antioxidant activity of 89.24%, while AuNPs showed 70.46% activity at 2.677 mg/mL. In comparison, the standard antioxidant Trolox demonstrated 91.19% inhibition at a concentration of 0.012 mg/mL. The IC_{50} values of green-synthesized AgNPs, AuNPs, and standard Trolox were calculated as 1.151, 1.485, and 0.006 mg/mL, respectively. The results obtained from this study indicate that biologically synthesized AgNPs and AuNPs can be effectively used as potent antioxidants.

Keywords Green tea · AgNPs · AuNPs · SFE · Uv–vis · FTIR · TEM · XRD

Introduction

Nanotechnology is the design, development, and use of components. Currently, the field of nanotechnology is multidisciplinary and includes elements of physics, chemistry, biology, and engineering [1, 2]. Inorganic and organic structures with sizes ranging from 1 to 100 nm are known as nanoparticles (NPs), and they can be created using physical, chemical, and, more recently, green synthesis techniques [3]. Scientists are interested in the potential biological and food-related applications of nanoparticles because of their size, distinctive structural shape, and optoelectronic and chemical characteristics [4–7]. Several nanostructures have been extensively researched for their potential use in cancer therapy and detection. These include carbon nanotubes, polymeric nanoparticles, metallic nanoparticles, microbially produced nanoparticles, liposomes, and magnetic nanoparticles [8]. A wide range of biological and medical systems can be altered by nanoscience in novel ways. According to predictions, nanotechnology will significantly impact the

✉ Gönül Serdar
gonulserdar@ktu.edu.tr

[1] Department of Central Research Laboratory, Karadeniz Technical University, 61080 Trabzon, Turkey

[2] Department of Chemistry, Faculty of Science, Karadeniz Technical University, 61080 Trabzon, Turkey

[3] Vocational School of Health Services, Artvin Çoruh University, 08000 Artvin, Turkey

Published online: 19 June 2025

future of biology and medicine [9]. Over the years, nanoparticles have emerged as key components in modern medicine, finding applications in diverse areas such as gene delivery and medical imaging. Their nanoscale dimensions result in a significantly increased surface area-to-volume ratio, which enhances their functional efficiency. One of the major advantages of nanoparticle technology lies in its ability to reduce poorly soluble drug particles from the microscale to the nanoscale, thereby improving their solubility and bioavailability [9].

Green synthesis is regarded as a promising approach for the production of nanoparticles, as it utilizes cost-effective and non-toxic raw materials [10]. This method offers a sustainable alternative due to its high therapeutic efficacy, low toxicity, target-specific binding capacity, and site-directed delivery potential. Furthermore, it poses no significant risk to either the environment or human health, positioning it as a safer and more environmentally friendly alternative to conventional synthesis techniques [11, 12]. The main objective of green nanotechnology is to reduce the hazards that nanotechnology-related products pose to the environment and human health in the near future and to encourage the replacement of current products with more ecologically friendly nanoproducts [8]. Nanotechnology and green chemistry combine to produce eco-friendly nanoparticles by using microorganisms, plants, and other natural processes to solve the toxicity issue [13]. With the use of safe, non-toxic, and environmentally sound "green chemistry" techniques, scientists have produced a variety of synthetic approaches for the production of nanoparticles, indicating a considerable benefit to nature and the environment [14]. The use of natural plants and microorganisms, such as bacteria, plants, yeasts, fungus, algae, diatoms, and metallic NPs like gold, silver, iron, and copper [15, 16], as well as their superior material and adaptable functioning, is made possible by the green synthesis approach. Due to their quick and cost-effective synthesis, stability of NPs in spherical shape, and tiny size, plant-derived metallic NPs are the favored synthesis method. Several plant extracts have been utilized in the past to create metallic nanoparticles, including seeds, fruit bark, seed powder, bran, and leaves [17]. Plant extract therefore eliminates many steps, lowers costs, and uses fewer chemical reagents by substituting organic solvents and chemical compounds in aqueous media [18]. According to reports, plants are far more efficient at reducing metal ions than microorganisms are at doing so, and they also produce more stable metal NPs [19]. By adjusting variables like pH, temperature, and reaction time, plants can modify and control the size and shape of NPs they produce. Magnesium, copper, gold, zinc, silver, and selenium are just a few examples of the different types of nanomaterials [20]. The most discussed environmentally friendly method to produce silver and gold nanoparticles is the biological reduction process. Green chemistry is the process by which AgNPs and AuNPs are produced by biological reduction [21]. In recent years, the swift progress of nanotechnology has ushered in a new era in materials science, enabling wide-ranging applications in the physical and chemical sciences, as well as in fields such as biology, electronics, medicine, catalysis, optics, and bioengineering [22, 23]. Among various noble metal nanoparticles, AgNPs have attracted considerable attention due to their diverse biomedical properties, including antioxidant, antibacterial, anti-angiogenic, wound healing, anti-inflammatory, and anticancer activities [22, 24]. Silver, in particular, has gained recognition for its well-established medicinal benefits [22, 25]. Currently, the green synthesis of AgNPs using medicinal plant extracts is being increasingly explored for its promising therapeutic potential [22, 26]. In the synthesis of nanoparticles, functional groups from green resources, such as hydroxyl groups, have reductive roles [27]. The plant extract serves as a stabilizing, capping, or both agent as well as a potent reducing agent in the one step and one-pot reaction that produces AgNPs in the nanoparticle production process [28]. Due to the electrical, optical, and magnetic properties of AgNPs, they are employed in healthcare and pharmaceuticals, particularly as a delivery system for drugs that fight cancer. The fact that it is antibacterial is its most significant benefit, particularly because it weakens bacterial cell walls and inhibits bacterial cell growth. AgNPs are also utilized in a variety of other goods and processes, including composite fibers, superconducting materials, biosensor materials, cosmetics, electronic components, and antibacterial applications [29]. Most of the NPs made from extracts of plants had spherical sizes from 5 to 100 nm, along with antimicrobial and anticancer properties. Leaf extracts have medicinal potential and antibacterial action because they include natural reducing phenolic substances, amino acids and vitamins [18]. Gold nanoparticles are gaining attention from researchers as potential cancer therapeutic and diagnostic metal NPs. AuNPs can be readily produced in a variety of shapes and sizes by adjusting the constituents and concentrations [30–32]. Additionally, AuNPs have demonstrated a notable improvement in the treatment of bacterial infections and inflammatory illnesses [33, 34]. One of the greatest options for the large-scale production of AuNPs with well-defined size and morphology is the plant-based green synthesis technology because of its reasonable cost [35]. Au is thought to be an appropriate metal for the synthesis of stable nanoparticles. It has been discovered that the majority of the physical characteristics of inorganic nanoparticles depend on their size and form. The unique optical and physical characteristics of AuNPs make them useful in a variety of sectors [36].

Green synthesis, on the other hand, is an environmentally beneficial method of producing AuNPs from the plant. A variety of plant components, including leaves, bark, stems,

roots, and others, are utilized as sources in the biosynthesis of AuNPs from the plant. These parts are chopped into small pieces and cooked in distilled water to produce an extract. One can purify the extract by centrifuging and filtering it. Metal ions are reduced from a mono- or divalent oxidation state to a zero-valent state by the bioreduction mechanism. Following that, the reduced metal atoms nucleate [37]. Finally, utilizing a one-pot, single-step, environmentally benign process, the extract-containing metallic salt solution is reduced from $Au^{+3}$to Au^{0}, and the synthesis of AuNP can happen in a matter of minutes to hours [24]. This morphology is caused by variations in the composition and concentration of reducing agents in plant extracts. Initial identification of synthesized AuNPs was made using a UV–vis spectrophotometer study of the reaction color change. The size, form, and distribution of the gold nanoparticles were seen by TEM images, and their crystalline structure was verified by DLS, XRD, and SAED. The capping ligands of the nanoparticles are functional groups such as –C–O–C–, –C–O–, –C = C–, and –C = O, as demonstrated by FTIR analysis [38]. The main objective of green nanotechnology is to reduce the hazards that nanotechnology-related products pose to the environment and human health in the near future and to encourage the replacement of current products with more ecologically friendly nanoproducts. The green synthesis of AuNPs can benefit several areas of science and technology, including green separation, green photocatalyst, drug delivery, anti-microorganism, adsorbent, detector, and anti-microorganism [27]. Recent years have seen a broad increase in the use of nanotechnology in a variety of industries, including but not limited to medicine, cosmetics, medical devices, electrical and electronic, pharmaceutical, food, and packaging. Green produced AuNPs have been demonstrated in preliminary experiments to have a variety of biological properties, including antioxidant, antiviral, antibacterial, and anticancer activities [8]. The three major classes of biomolecules found in tea are catechins, phenolic acids, and alkaloids. While each of these constituents has a specific bioactivity, a combination of them often exhibits a synergistic effect. It is important to note that the pharmacological effects of tea are caused by catechins and phenolic acids [39]. For the natural production of nanoparticles, green tea has been utilized [40, 41]. Green tea's main constituents are reducing and coating substances known as EGC, epigallocatechin-3-gallate (EGCG), EC, and epicatechin-3-gallate (ECG) [42, 43] Recent research indicates that Bergal et al. [3] tested the surface plasmon resonance with UV spectrophotometric investigations at various time intervals by adjusting the concentration of reducing agent (1–5–10–20 mM) at varied concentrations using 5 g of fresh green tea leaves. The other characterization investigations of AgNP synthesis were carried out at room temperature because the greatest SPR absorption peak at 413.67 nm was attained there in an hour. AgNPs were discovered by TEM and SEM research to have been synthesized in a variety of forms, including spherical, hemispherical, and ellipsoidal [3]. The highest rise in absorbance at 423 nm of silver nanoparticles produced using 5 g *Camellia sinensis* and 1 mM $AgNO_3$ was observed after 96 h, according to Flieger and colleagues [44]. Also, they discovered that after 72 h, the nanoparticle population became more scattered despite being more uniform at first.

In a previous study conducted in 2017, two distinct extraction strategies were developed for the recovery of bioactive compounds from tea leaves [45]. In the first approach, green tea extract was obtained by directly extracting the leaves into a citric acid containing aqueous medium under microwave-assisted conditions. In the second strategy, catechins were isolated through a simple liquid–liquid extraction procedure. The isolated catechins were subsequently employed in the synthesis of AgNPs using a microwave-assisted method [45]. In a subsequent study published in 2023, sequential MAE and SFE techniques were applied to green tea samples collected from the Eastern Black Sea region [46]. The resulting catechin-rich extracts were successfully utilized for the green synthesis of AuNPs via microwave irradiation [46]. The present study aims to further advance these findings by synthesizing both Ag and Au nanoparticles under varying temperature conditions (25 °C, 35 °C, and 45 °C), using aqueous catechin extracts obtained through sequential MAE and SFE from green tea leaves harvested from the same (Eastern Black Sea) region. In alignment with green chemistry principles, the synthesis process was intentionally developed to minimize environmental impact. The resulting nanoparticles are comprehensively characterized using TEM, XRD, FT IR, and zeta sizer analysis to elucidate their morphological, structural, and surface properties.

Material and Methods

Preparation of Catechin Extract

Green tea samples were sourced from the Trabzon Province, Türkiye, and subsequently dried at ambient temperature in a shaded environment to preserve their phytochemical integrity. For the extraction of catechins, a modified microwave-assisted extraction protocol was employed based on previously reported methodologies [47]. Specifically, 10 g of dried green tea leaves was immersed in 200 mL of a 1:1 (v/v) aqueous solution comprising 0.1 M citric acid and distilled water. The mixture was initially left to stand for 90 min to facilitate pre-extraction soaking, followed by microwave treatment in a laboratory grade microwave oven at 600 W power and 80 °C for 4 min [46]. The resulting extract was subjected to freeze-drying to

ensure complete removal of solvents prior to the subsequent SFE step. Catechin-rich fractions were isolated via a modified CO_2-SFE process utilizing ethanol as a co-solvent at a flow rate of 0.5 mL/min. The extraction was conducted under pre-optimized conditions: 250 bar pressure, 60 °C temperature, and a total extraction time of 3 h [48]. The final catechin extract solution was prepared at a concentration of 2% (w/v) and employed in nanoparticle synthesis procedures.

Synthesis of AgNPs and AuNPs

AgNPs and AuNPs were successfully biosynthesized using catechin extract derived from the SFE process, which served simultaneously as a reducing and stabilizing agent. Aqueous solutions of $AgNO_3$ (1 mM) and $HAuCl_4.3H_2O$ (0.5 mM) were prepared in separate flasks. To these, varying volumes (0.5, 1, 2, 3, and 4 mL) of the catechin extract solution (2% w/v) were added individually to a fixed volume of 100 mL of each precursor solution. The reaction mixtures were incubated at three different temperatures (25, 35, and 45 °C) for variable durations to determine the optimal synthesis conditions. The synthesis of AgNPs was visually confirmed by a color shift from light yellow to brown, whereas the formation of AuNPs was indicated by the appearance of a distinctive dark purple color emerging from the initially light yellow solution. The time required for the emergence of these colors and the stability of the colloidal dispersions were systematically recorded. Each synthesis condition was repeated three times to ensure reproducibility and statistical relevance of the findings.

Characterization of AgNPs and AuNPs

The biosynthesized AgNPs and AuNPs were comprehensively characterized using TEM, FTIR, UV–Vis, XRD, and DLS analysis using a zeta-sizer. To confirm the formation of AgNPs and AuNPs synthesized using catechin, UV–Vis spectrophotometric analysis was performed (Shimadzu UVP-1240, Japan). The absorbance spectra were measured within the wavelength range of 300–800 nm. To ensure reproducibility, three independent biosynthesis experiments were performed. The crystalline structure and phase purity of the synthesized nanoparticles were analyzed using an X-ray diffraction spectrometer (Panalytical X'Pert^3 Powder XRD) equipped with monochromatic Cu Kα radiation. Scanning was carried out over a 2θ range of 10° to 90°. Functional groups involved in the reduction and stabilization of nanoparticles were identified by FTIR spectroscopy (PerkinElmer Frontier) within the spectral range of 4000–500 cm^{-1}. Morphological features and size distribution of AgNPs and AuNPs were further analyzed via high-resolution transmission electron microscopy (TEM, Hitachi HT-7700) operated at an accelerating voltage of 40–120 kV. A Malvern Zetasizer Nano ZSP Analyzer was employed to determine the nanoparticles' hydrodynamic diameter, PDI, and zeta potential. Measurements were carried out within a controlled temperature range of 0 °C to 90 °C with ±0.1 °C accuracy to assess colloidal stability.

Antioxidant Activity

The antioxidant potential of the biosynthesized AgNPs and AuNPs was assessed using the 2,2-diphenyl-1-picrylhydrazyl (DPPH) radical scavenging assay, as described by Molyneux [49]. For the analysis, 0.75 mL of the nanoparticle extract at varying concentrations was mixed with 0.75 mL of a 0.1 mM DPPH solution prepared in methanol.

The reaction mixtures were incubated at room temperature in the dark for 50 min to allow for radical scavenging activity. The decrease in absorbance, indicating the extent of DPPH radical scavenging, was measured at 517 nm using a UV–Vis spectrophotometer, with methanol serving as the blank. All measurements were performed in triplicate to ensure reproducibility. The antioxidant capacity of the samples was expressed in terms of IC_{50}, defined as the concentration of the extract required to inhibit 50% of the DPPH radicals (mg/mL).

Results and Discussions

AgNP and AuNP Production with Catechin Extract

As illustrated in Fig. 1a, a well-defined SPR peak is observed, corresponding to the successful synthesis of catechin-AgNPs. In contrast, the control sample containing only $AgNO_3$, in the absence of any plant-derived extract, exhibits no such optical feature. Similarly, Fig. 1b demonstrates a characteristic SPR peak indicative of catechin-AuNPs in the presence of catechin extract, whereas no corresponding peak is observed in the control sample consisting solely of $HAuCl_4 0.3H_2O$. These spectroscopic observations provide compelling evidence that nanoparticle formation is exclusively driven by the reducing potential of catechin molecules. To exclude the possibility that nanoparticle formation resulted from abiotic processes such as thermal decomposition or spontaneous reduction, control experiments were conducted using $AgNO_3$ and $HAuCl_4 \bullet 3H_2O$ solutions in the absence of catechin extract, as shown in Fig. 1a and b. The absence of any detectable SPR peaks in these control groups, as evidenced by the spectral data in Fig. 1, strongly supports the conclusion that nanoparticle synthesis in the experimental groups is driven solely by the catechin-mediated reduction mechanism.

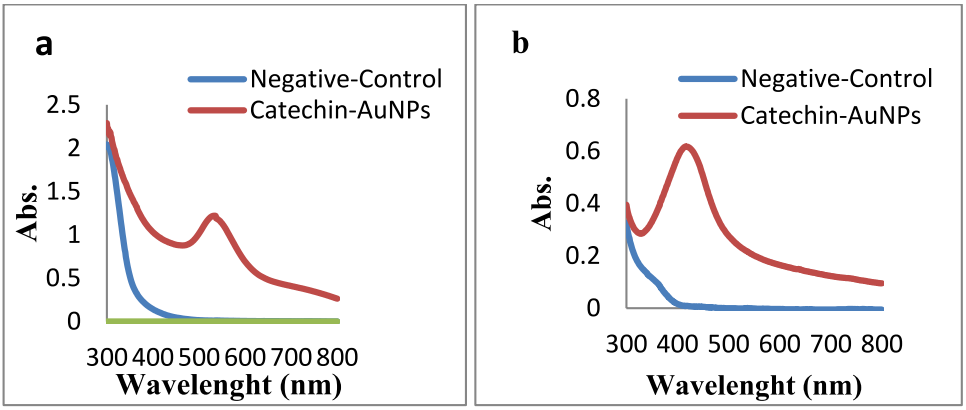

Fig. 1 **a** SPR peak of Catechin-AgNPs (compared with extract-free control group). **b** SPR peak of Catechin-AuNPs (compared with extract-free control group)

Depending on the amount and duration of exposure to catechin extract solutions, the color of the solutions changed from light yellow to brown for AgNPs (Fig. 2a) [45, 50–53] and from light yellow to dark purple for AuNPs (Fig. 5a) [54–57]. The excitation of Ag and Au nanoparticles' surface plasmon vibration is what causes the production of Ag and Au nanoparticles as a color change. Different volumes of 1 mM AgNO3 and 0.5 mM HAuCl4.3H2O solutions were mixed separately with 0.5 to 4 mL catechin extract solutions in a magnetic stirrer at different temperatures (25, 35, 45 °C). Then, absorbances were measured on a UV spectrophotometer between 1 and 240 min for AgNPs (Figs. 2, 3, and 4) and 1 to 60 min for AuNPs (Figs. 5, 6, and 7). The effects of temperature and volume changes on AgNP and AuNP synthesis were determined by observing the SPR absorption peaks (Figs. 2, 3, 4, 5, 6, and 7). In experiments performed at temperatures of 25, 35, and 45 °C for the synthesized silver and gold nanoparticles, narrow peaks with the highest absorption were obtained at 25 °C. Characteristic plasmon resonance peaks ranging from 400 to 460 nm for silver nanoparticles and 500 to 600 nm for gold nanoparticles [46] were found by scanning the samples from 300 to 800 nm (Shimadzu, Japan), and the strength and length of the resulting peaks were correlated with the particle size distribution.

In this study, a shift toward longer wavelengths in the λmax values was observed with increasing temperature and extract concentration. Furthermore, peak broadening was found to be more pronounced at elevated temperatures (35 °C and 45 °C) and higher extract volumes (1–4 mL). These findings reveal the critical impact of synthesis parameters on the optical properties of AgNPs, emphasizing that temperature and reducing agent concentration must be precisely controlled in order to obtain monodisperse nanoparticles with narrow and well-defined SPR characteristics. The synthesis of AuNPs using catechin extract exhibited a distinct SPR band in the range of 500–600 nm. As the volume of catechin extract increased from 0.5 to 4.0 mL, a significant increase in SPR peak intensity was observed, accompanied by a shift in the λ_max value. The data clearly show that both temperature and catechin concentration have significant effects on the optical properties and stability of the synthesized AgNPs and AuNPs.

As shown in Figs. 2a and 5a, AgNPs and AuNPs were successfully synthesized at 25 °C using 0.5 mL of catechin extract in aqueous solutions of 1 mM $AgNO_3$ and 0.5 mM $HAuCl_4 0.3H_2O$, yielding maximum absorbance values of 2.066 and 1.454, respectively. These results indicate that the optimal synthesis conditions for both nanoparticle types involved the use of 0.5 mL catechin extract with 1 mM $AgNO_3$ for AgNPs and 0.5 mM $HAuCl_4 \bullet 3H_2O$ for AuNPs. Given that the most intense and well-defined SPR peaks were obtained at 25 °C under these conditions, subsequent characterization studies were conducted using the nanoparticles synthesized at this temperature. These findings suggest that the synthesis occurring at 25 °C is likely under kinetic control, which favors slower nucleation and growth rates, thereby promoting the formation of smaller and more uniformly shaped nanoparticles. In contrast, at higher temperatures (35 °C and 45 °C), the tendency for particle growth and aggregation increases, leading to broader SPR peaks and, consequently, greater polydispersity—indicating heterogeneity in particle size and morphology.

In our previous study, we also reported that bioactive compounds with reducing properties exhibit optimal activity within certain concentration ranges; exceeding these limits may reduce their effectiveness or result in adverse effects such as nanoparticle instability and irregular morphologies [45]. Therefore, the superior results obtained under lower extract volumes and mild temperatures in this study can be attributed to a more balanced and controlled reduction environment. This finding highlights the importance of optimizing not only the type of reducing agent but also its concentration and the thermal conditions in green synthesis protocols. The synthesized AgNP and AuNP colloidal solutions were stored under refrigerated conditions, and their UV–Vis absorption spectra were monitored over

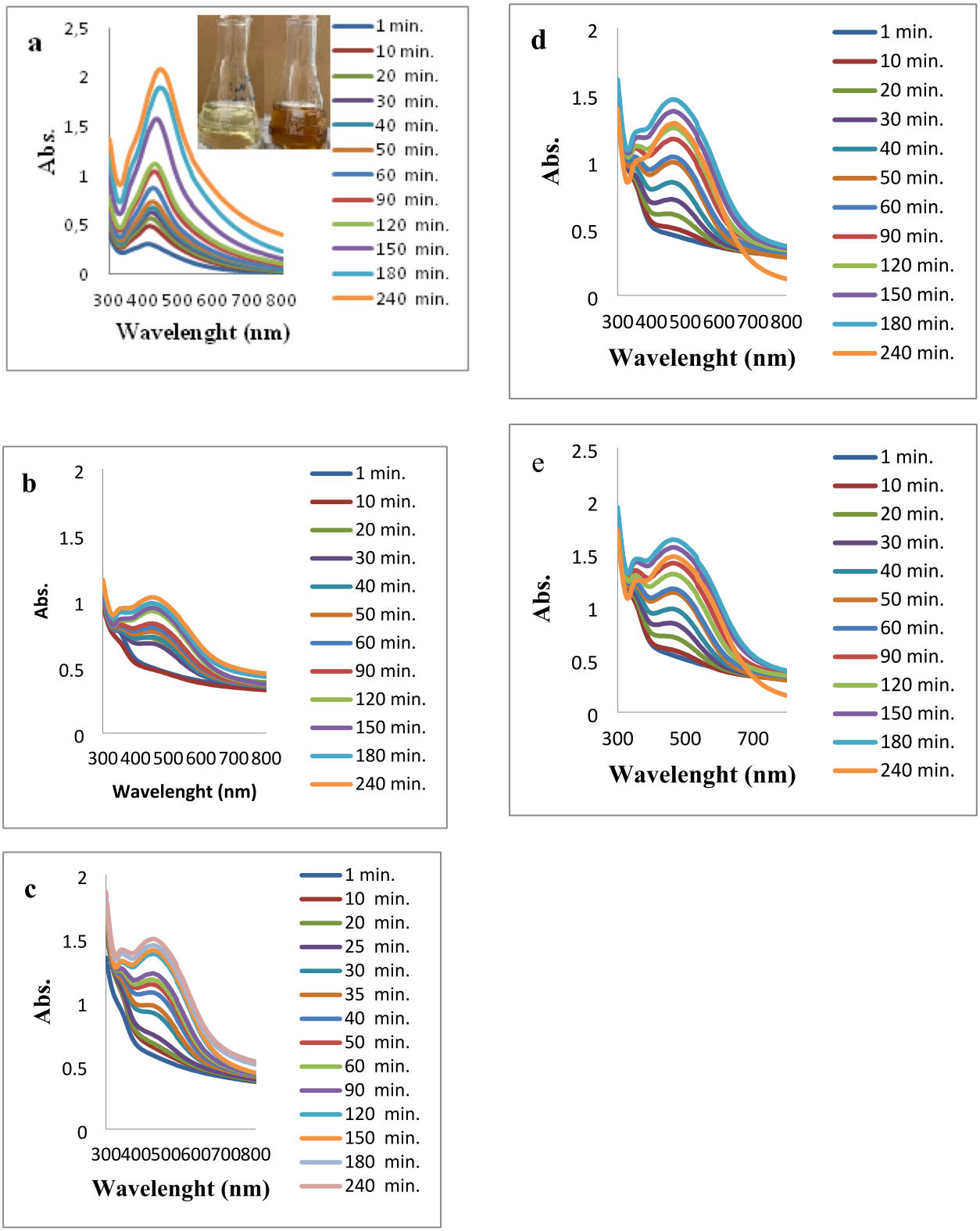

Fig. 2 UV–vis spectra of Ag nanoparticles synthesized with 1 mM $AgNO_3$ and in different volumes of catechin extract at 25 °C (**a** 0.5 mL, **b** 1 mL, **c** 2 mL, **d** 3 mL, **e** 4 mL)

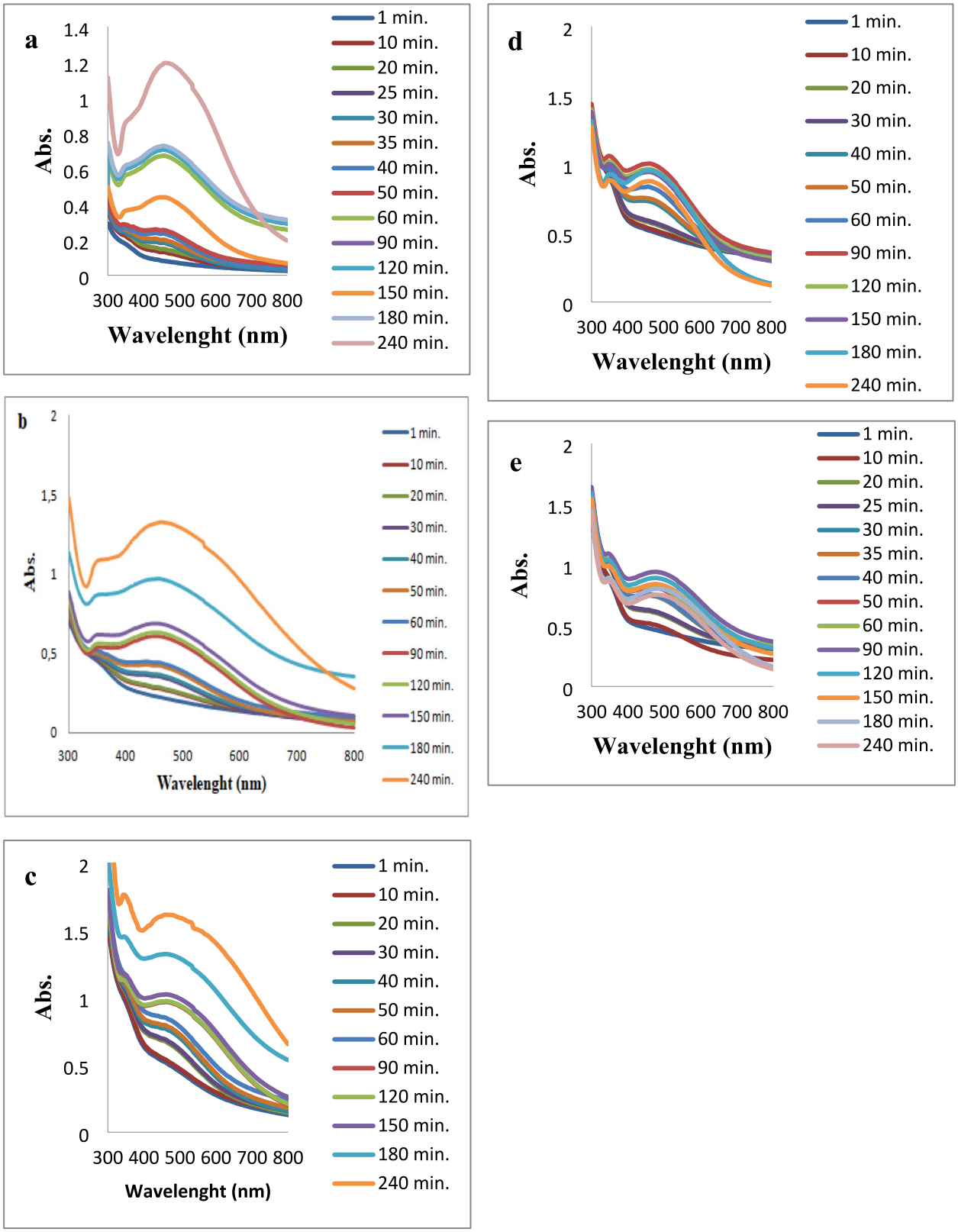

Fig. 3 UV–vis spectra of Ag nanoparticles synthesized with 1 mM $AgNO_3$ and in different volumes of catechin extract at 35 °C (**a** 0.5 mL, **b** 1 mL, **c** 2 mL, **d** 3 mL, **e** 4 mL)

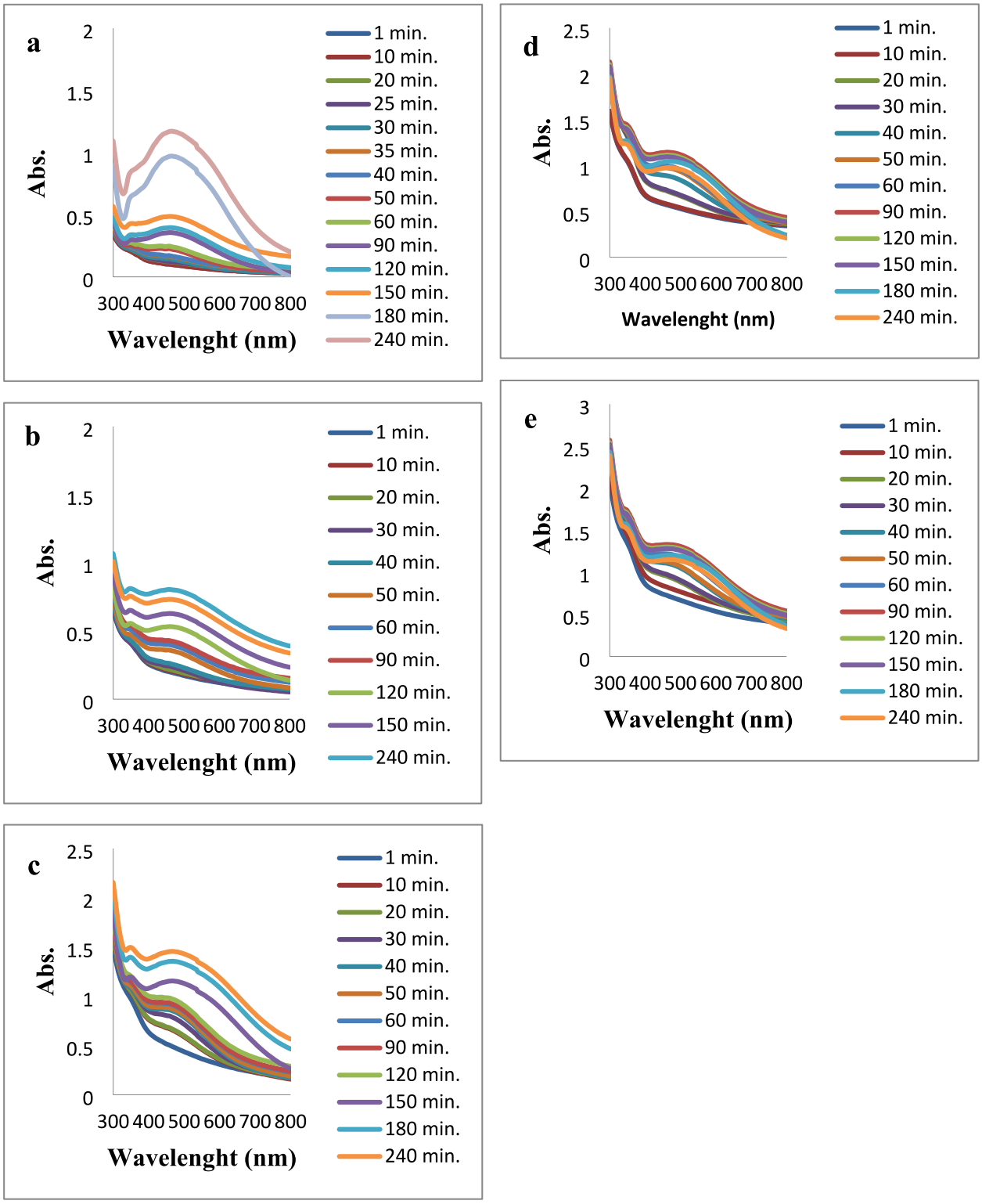

Fig. 4 UV–vis spectra of Ag nanoparticles synthesized with 1 mM $AgNO_3$ and in different volumes of catechin extract at 45 °C (**a** 0.5 mL, **b** 1 mL, **c** 2 mL, **d** 3 mL, **e** 4 mL)

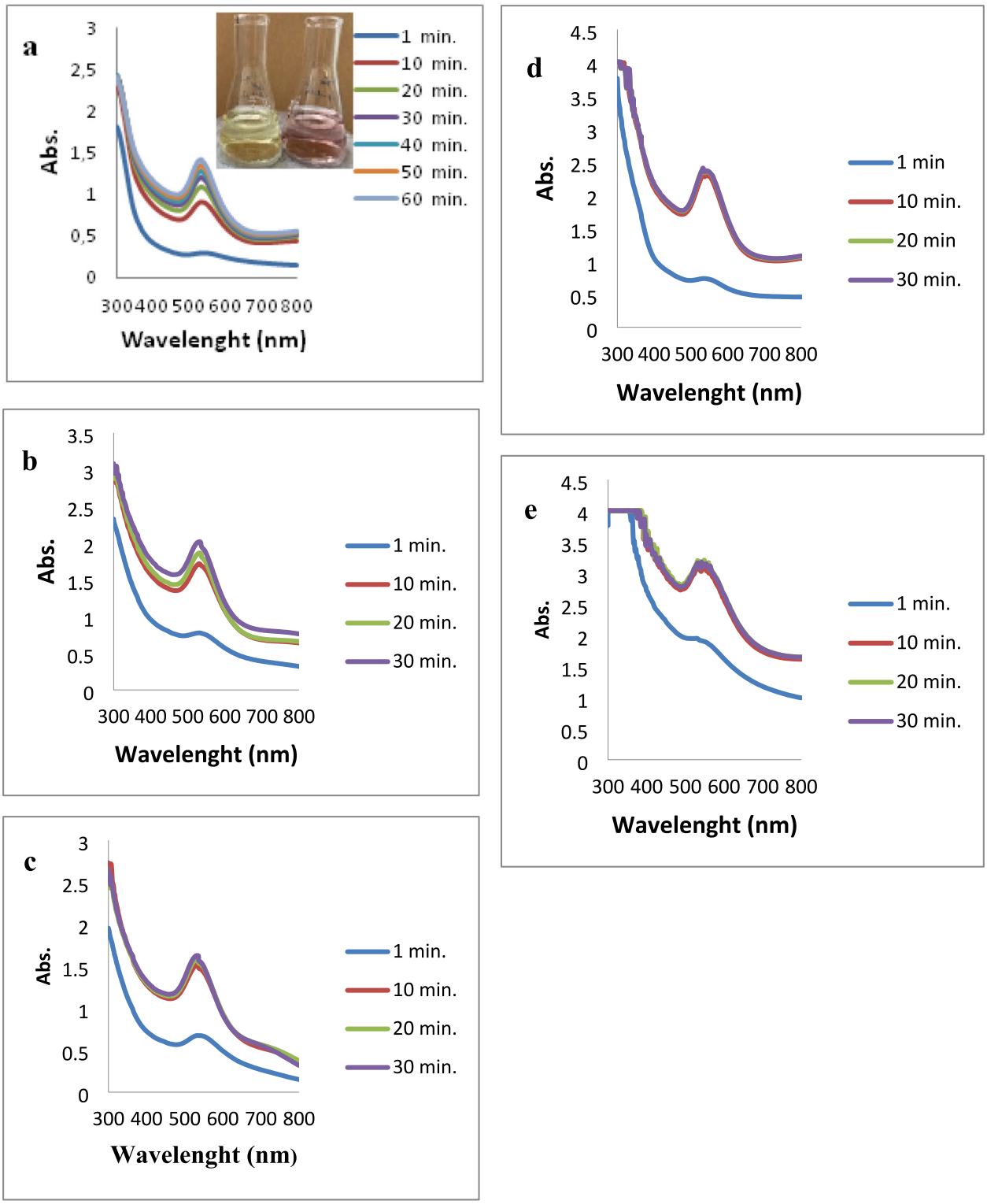

Fig. 5 UV–vis spectra of Au nanoparticles synthesized with 0.5 mM $HAuCl_4.3H_2O$ and in different volumes of catechin extract at 25ºC [a)0.5 mL, b)1 mL, c) 2 mL, d)3 mL, e)4 mL]

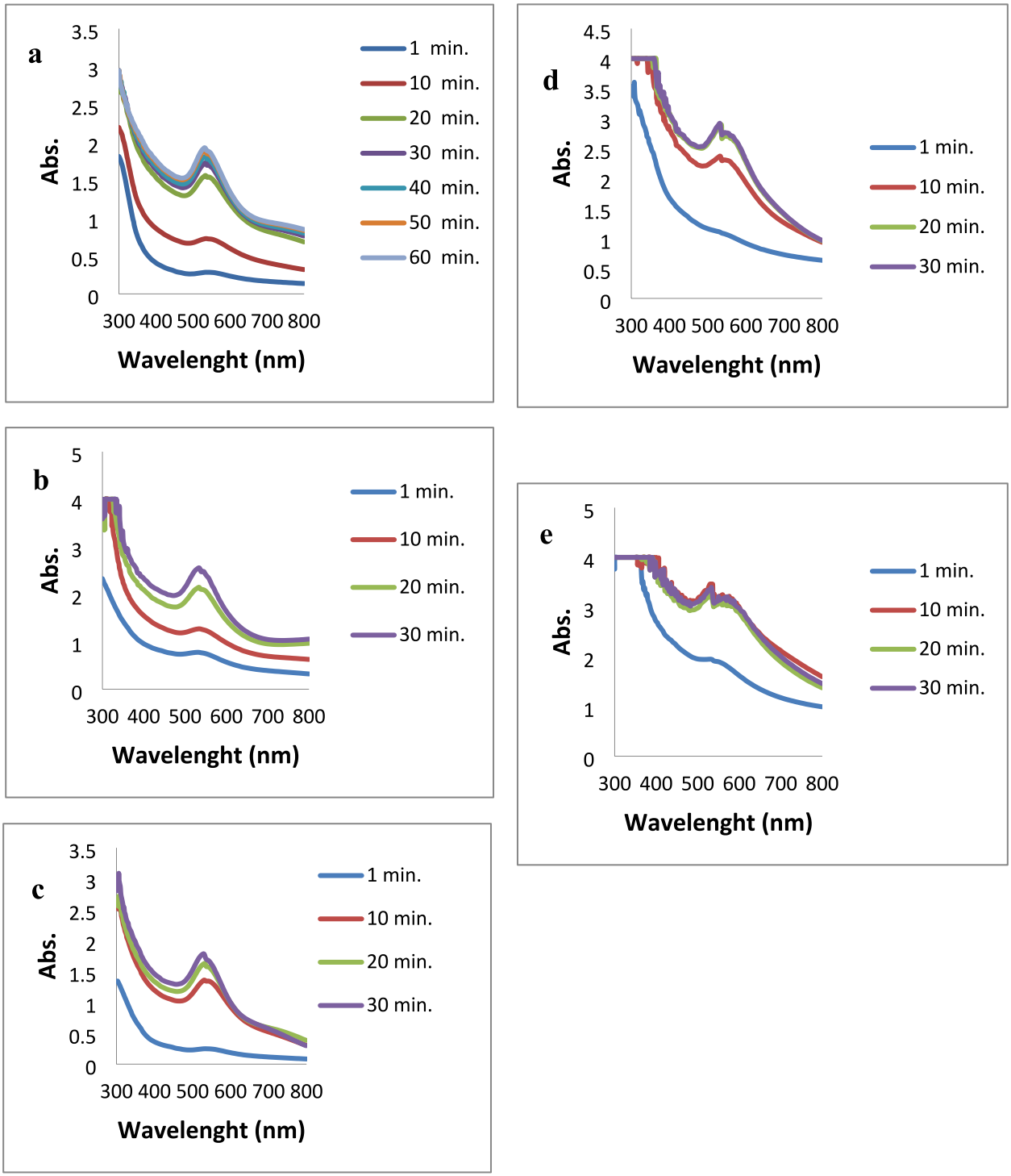

Fig. 6 UV–vis spectra of Au nanoparticles synthesized with 0.5 mM $HAuCl_4.3H_2O$ and in different volumes of catechin extract at 35 °C (**a** 0.5 mL, **b** 1 mL, **c** 2 mL, **d** 3 mL, **e** 4 mL)

a period of 45 to 60 days. As previously reported by Serdar and Gül Kılınç [46] and Sökmen et al. [45], the nanoparticles remained stable throughout this storage period. In support of these findings, previous studies have demonstrated that AgNPs can be synthesized at room temperature using green tea and black tea extracts [3, 58], while gold nanoparticles have also been successfully produced under similar ambient conditions [59, 60].

In our previous study, effective extraction conditions for tea samples were reported. In that study, an aqueous

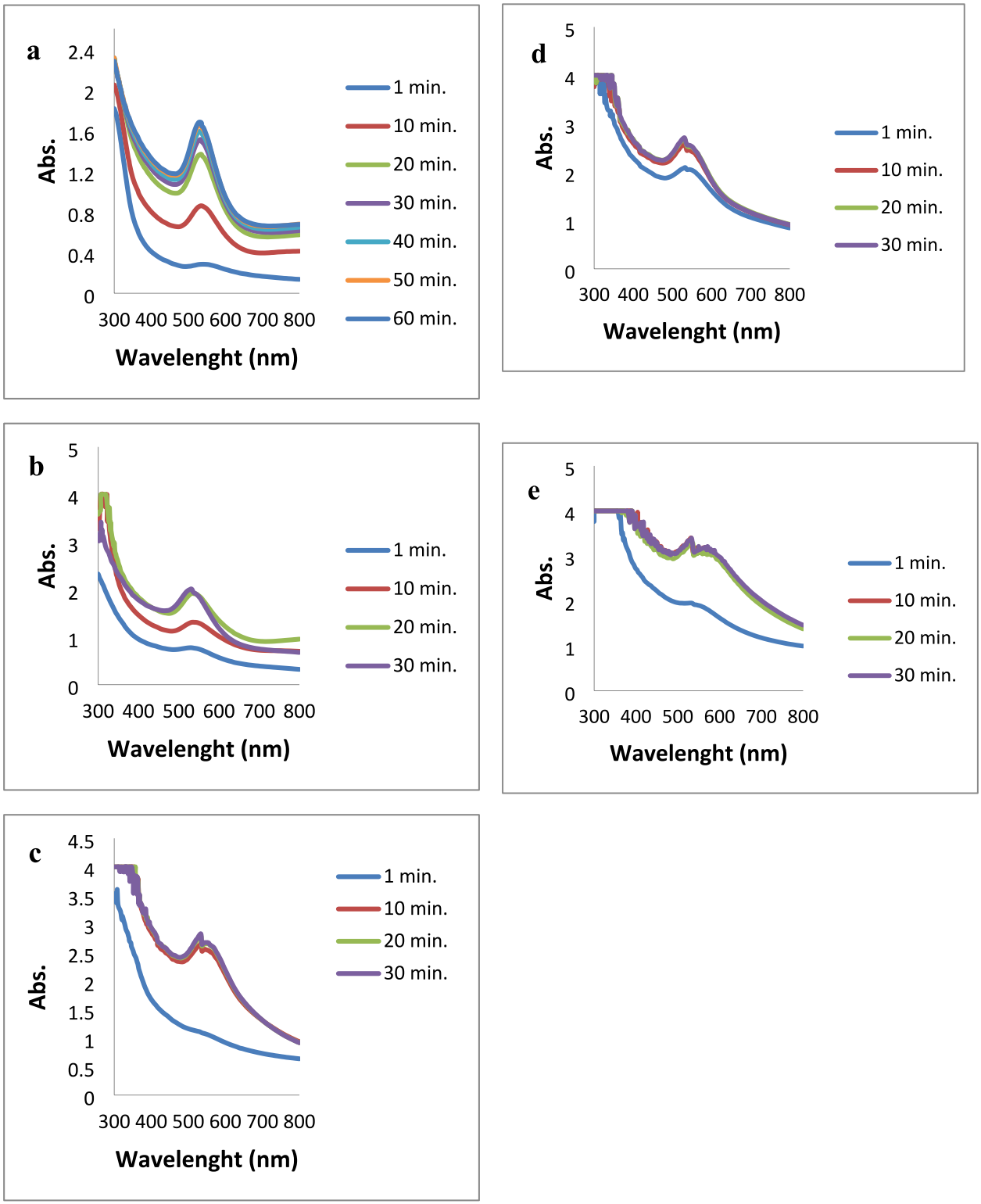

Fig. 7 UV–vis spectra of Au nanoparticles synthesized with 0.5 mM $HAuCl_4.3H_2O$ and in different volumes of catechin extract at 45 °C (**a** 0.5 mL, **b** 1 mL, **c** 2 mL, **d** 3 mL, **e** 4 mL)

citric acid solution was used as the extraction solvent in the MAE method, resulting in an extract with high phenolic content, particularly rich in catechins [61]. As stated in our previous works [45, 46], the presence of citric acid in the extraction medium also has a positive effect on the stabilization of nanoparticles. Therefore, in the present study, a citric acid–water solution was also used for the synthesis of nanoparticles.

Structural Analysis

The successful synthesis of AgNPs and AuNPs was validated through a comprehensive set of characterization techniques, including TEM, DLS, XRD, UV–Vis spectroscopy, and zeta potential analysis. The morphological features and structural formation of AgNPs and AuNPs are distinctly depicted in the TEM micrographs shown in Figs. 8 and 9, respectively.

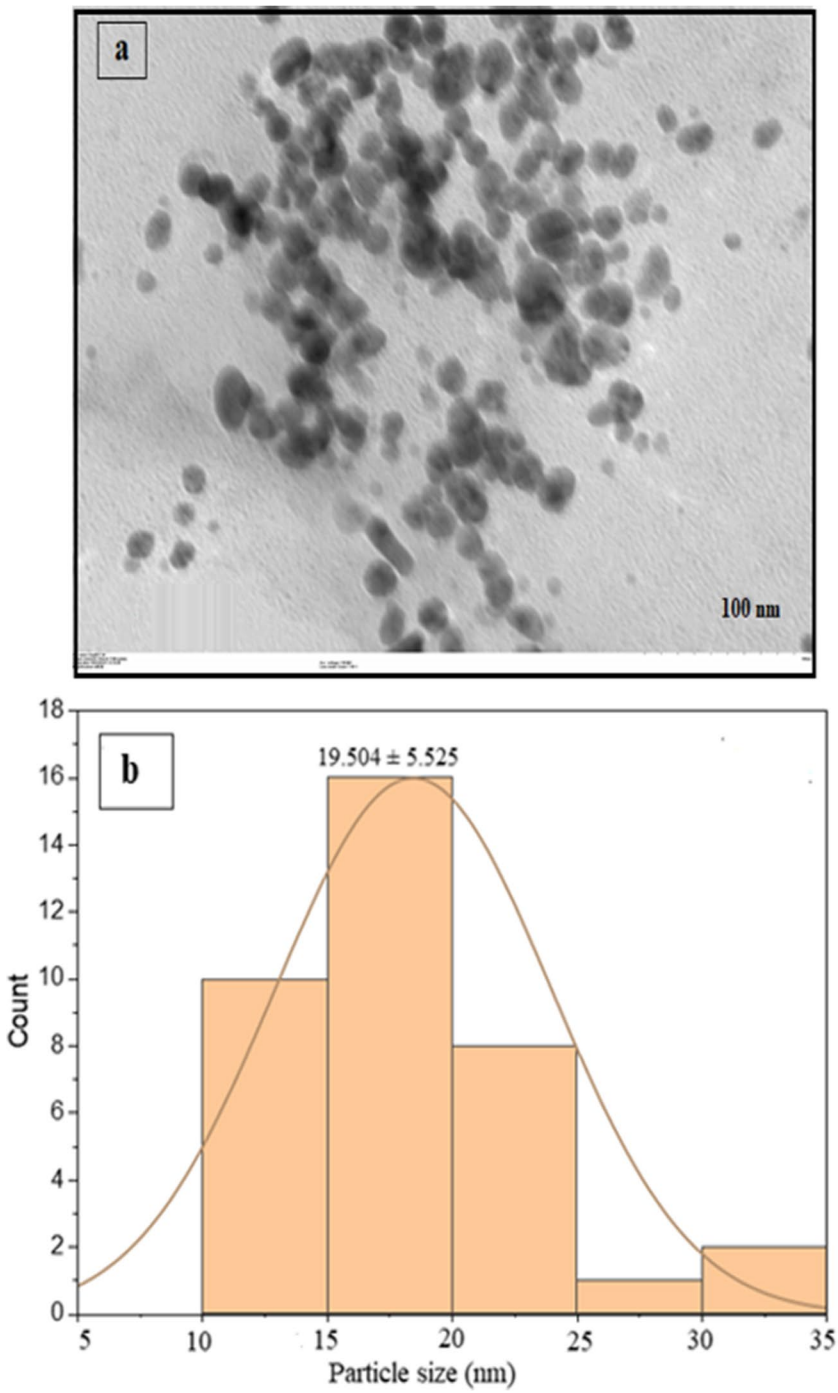

Fig. 8 **a** TEM images of Ag nanoparticles synthesized with 1 mM $AgNO_3$ and 0.5 mL catechin extract at 25 °C. **b** TEM distribution histogram

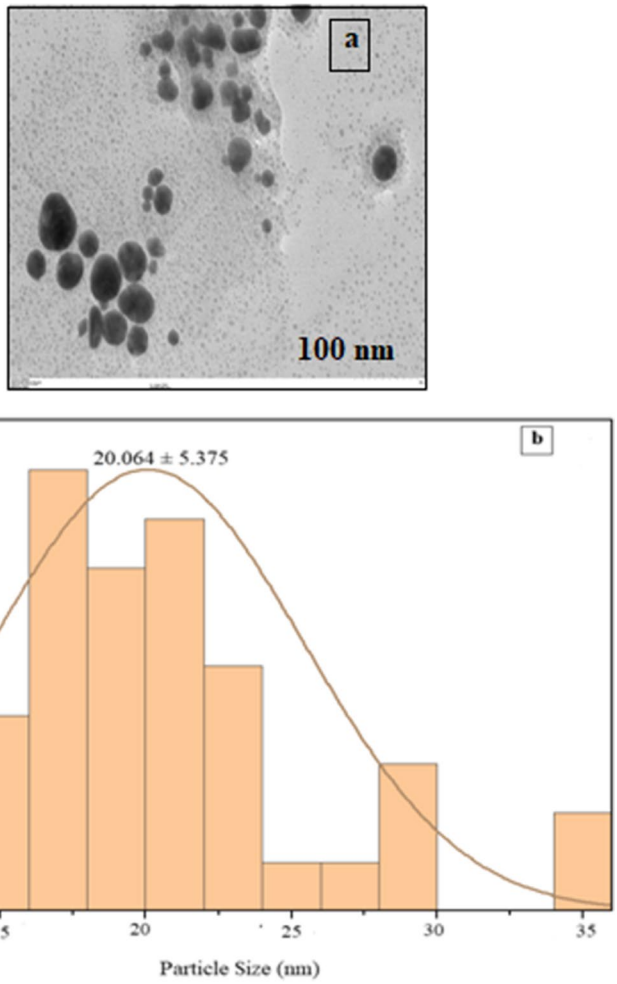

Fig. 9 **a** TEM images of Au nanoparticles synthesized with 0.5 mM $HAuCl_4.3H_2O$ and 0.5 mL catechin extract at 25 °C. **b** TEM distribution histogram

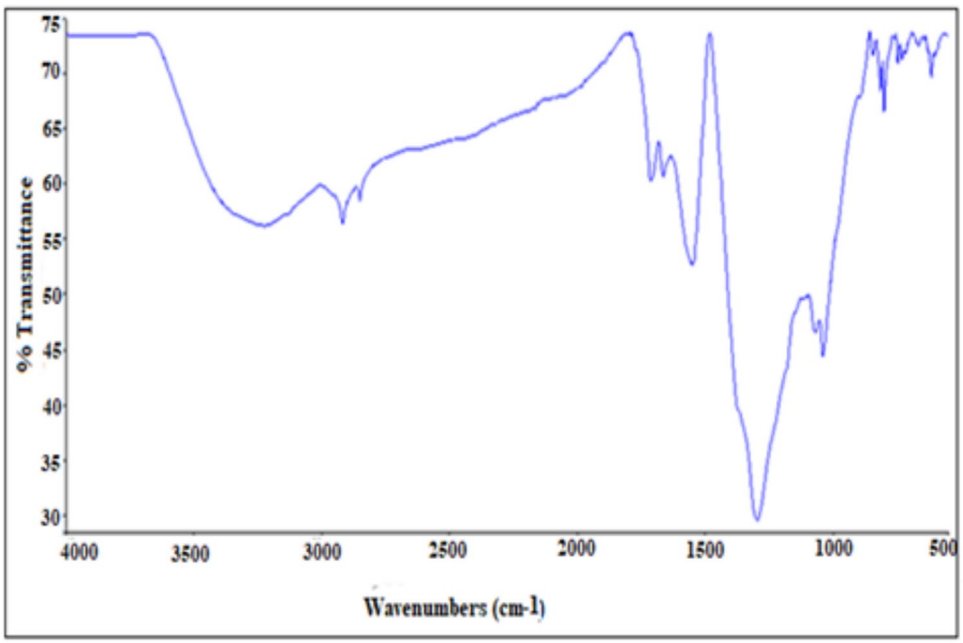

Fig. 10 FT-IR analysis spectrum of Ag nanoparticles produced with 1 mM $AgNO_3$ and 0.5 mL catechin extract at 25 °C

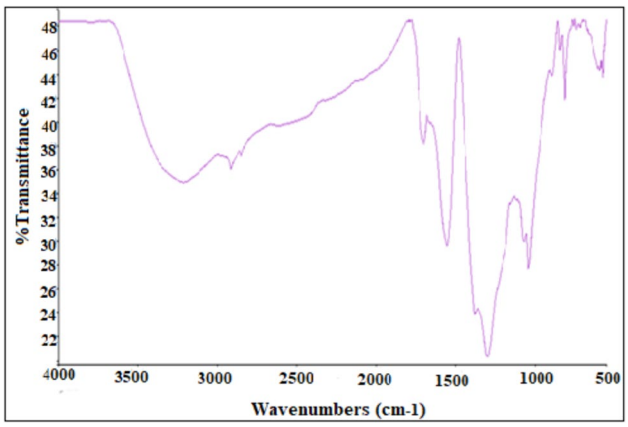

Fig. 11 FT-IR analysis spectrum of Au nanoparticles produced with 0.5 mM $HAuCl_4.3H_2O$ and 0.5 mL catechin extract at 25 °C

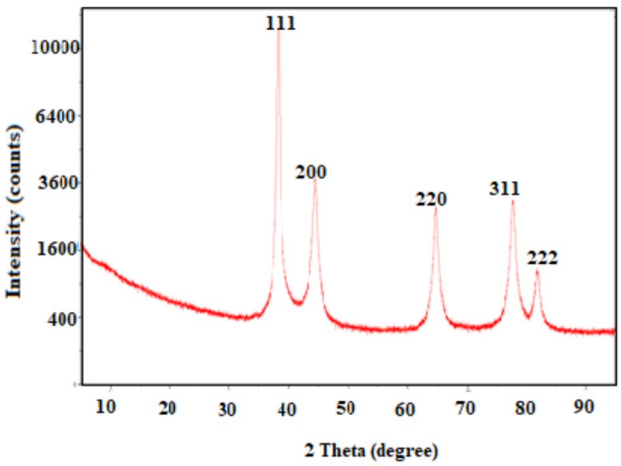

Fig. 13 XRD analysis result of Au nanoparticles synthesized with 0.5 mM $HAuCl_4.3H_2O$ and 0.5 mL catechin extract at 25ºC (diffraction peaks 2θ = 38.16°, 44.32°, 64.60°, 77.57°, and 81.61°), respectively)

The particle size distribution histogram obtained from TEM analysis (Fig. 8) indicates that the average diameter of the synthesized AgNPs is 19.504 ± 5.525 nm, with sizes ranging between 10.284 and 33.603 nm. Similarly, the histogram presented in Fig. 9 reveals that the average size of the AuNPs is 20.064 ± 5.375 nm, with particle sizes ranging from 11.748 to 34.705 nm. The TEM images shown in Fig. 8 and 9 confirm the successful synthesis of both AgNPs and AuNPs. Moreover, the observed nanoparticle morphologies are consistent with the SPR bands obtained from UV–Vis spectroscopic analysis. This morphological consistency highlights a strong correlation between particle shape and optical properties. Furthermore, the findings presented in Figs. 14 and 15 align well with existing literature, reinforcing the credibility of the analysis [3, 45, 46, 62].

The FTIR spectra presented in Figs. 10 and 11 provide important information about the presence of phenolic compounds on the surface of AgNPs and AuNPs synthesized from catechin extracts prepared by the SFE method at 25 °C. These spectra indicate the presence of phenolic carbonyl groups on the nanoparticle surfaces [45]. It is believed that these compounds were formed as a result of the oxidation of phenolic substances such as catechins during the reduction of silver and gold ions [45, 46]. We can understand the functional groups responsible for the reduction of Ag^{+1} to Ag^0 and Au^{+3} to Au^0 and the stabilization of the resulting silver and gold nanoparticles from the FTIR spectral analysis spectra of the relevant nanoparticles.

Fig. 12 XRD analysis result of Ag nanoparticles synthesized with 1 mM $AgNO_3$ and 0.5 mL catechin extract at 25 °C (diffraction peaks 2θ = 38.19°, 44.30°, 64.56°, 77.41°, and 81.92°, respectively)

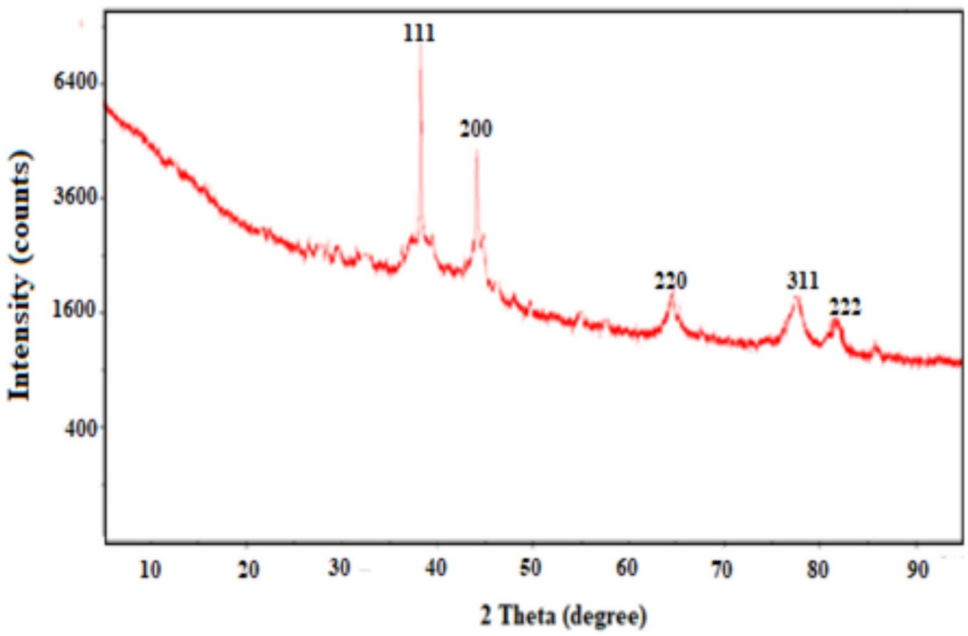

The presence of the characteristic diffraction peaks of Ag and Au observed in the XRD patterns aligns well with the standard reference data from the Joint Committee on Powder Diffraction Standards (JCPDS), corresponding to card numbers JCPDS: 04–0783 for metallic silver and JCPDS: 04–0784 for metallic gold. All diffraction patterns exhibit prominent peaks along the (111) crystallographic plane, indicating preferential crystal growth in this orientation for both AgNPs and AuNPs. Based on the Debye–Scherrer equation, the average crystallite size of the synthesized AgNPs was calculated to be 18.82 nm (Fig. 12), which is consistent with previously reported values in the literature [3, 45, 63]. Similarly, the gold nanoparticles displayed a crystalline structure, and their average crystallite size was estimated as 14.31 nm using the same equation (Fig. 13). This result is also in good agreement with earlier findings reported by Serdar and Gül Kılınç [46], Ghosh et al. [59], Geraldes et al. [60], and Jia et al. [64].

Figure 14a and b presents the characterization results of silver nanoparticles synthesized at 25 °C in an aqueous medium, revealing an average particle size of 37.61 ± 1.246 nm, a zeta potential of –20.4 ± 0.289 mV, and PDI of 0.271 ± 0.006.

As shown in Fig. 15a and b, gold nanoparticles synthesized at 25 °C in an aqueous medium exhibited an average particle size of 37.9 ± 0.2627 nm, a zeta potential of –22.6 ± 0.635 mV, and PDI of 0.295 ± 0.004. Moreover, the characterization results presented in Figs. 14 and 15 were found to be in good agreement with previously reported findings in the literature [44, 60, 63].

XRD analysis confirmed the crystalline structure of the synthesized AgNPs and AuNPs, with average crystallite sizes of approximately 18.82 nm and 14.31 nm, respectively (Figs. 12 and 13). However, particle size characterization by TEM revealed broader size distributions for both nanoparticle types. As shown in Figs. 8 and 9, the average particle sizes were measured to be 19.504 ± 5.525 nm for AgNPs (ranging from 10.284 to 33.603 nm) and 20.06 ± 5.38 nm for AuNPs (ranging from 11.75 nm to 34.71 nm), indicating a degree of polydispersity in both samples. Further analysis using DLS provided insight into the hydrodynamic behavior of the nanoparticles in aqueous media at 25 °C. The average hydrodynamic diameter was found to be 37.61 ± 1.246 nm for AgNPs (Fig. 14a–b) and 37.9 ± 0.26 nm for AuNPs (Fig. 15a–b). Zeta potential measurements revealed values of –20.4 ± 0.289 mV for AgNPs and –22.6 ± 0.64 mV for AuNPs, suggesting moderate colloidal stability in both cases. The PDI values were calculated as 0.271 ± 0.006 for AgNPs and 0.295 ± 0.004 for AuNPs, reflecting relatively narrow size distributions and acceptable uniformity for potential nanotechnological applications. The sequential increase observed from the crystallite sizes of AgNPs and AuNPs determined by XRD, to their physical dimensions observed via TEM, and finally to their hydrodynamic diameters measured by DLS, demonstrates the necessity of employing multiple, complementary characterization techniques to achieve a comprehensive understanding of the morphology and environmental behavior of AgNPs and AuNPs. These findings are also consistent with the relevant literature [45, 46].

Antioxidant Activity of AgNPs and AuNPs

The antioxidant activity of the synthesized materials was evaluated using the DPPH (2,2-diphenyl-1-picrylhydrazyl) assay, which measures radical scavenging based on the ability of compounds to donate hydrogen atoms and neutralize DPPH free radicals, leading to a measurable

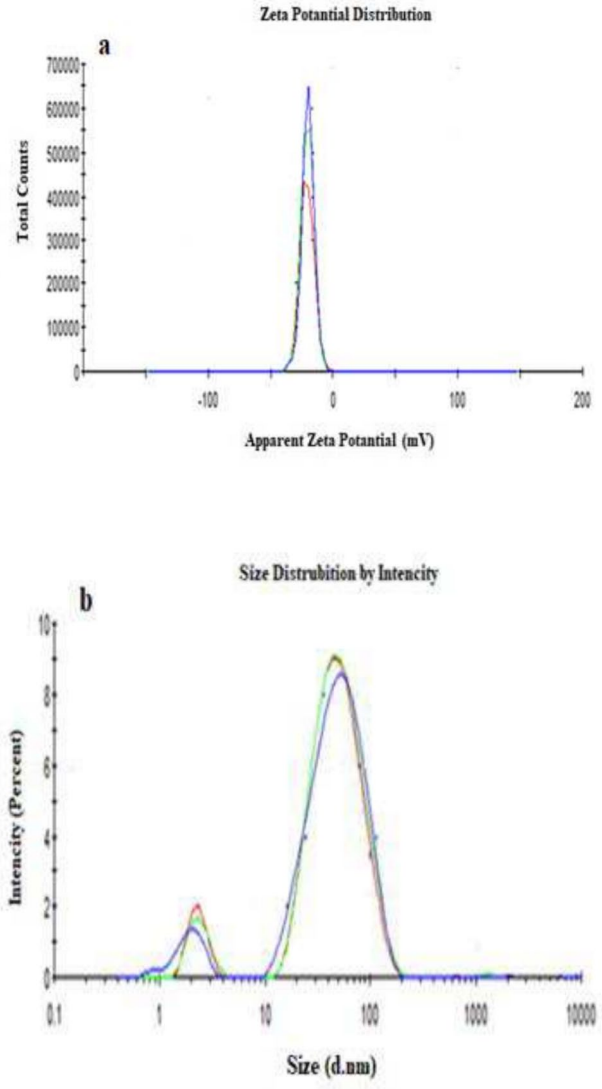

Fig. 14 **a** Zeta potential and **b** size distribution of Ag nanoparticles synthesized with 1 mM $AgNO_3$ and 0.5 mL catechin extract at 25 °C

decrease in absorbance [65]. In this test, antioxidative capacities of AgNPs and AuNPs were determined by their free radical scavenging potentials (SCA, % I) and IC_{50} values, all of which are given in Table 1 and also Fig. 16.

In the conducted DPPH assay, the IC_{50} values of the tested samples were found to range between 1.151 and 1.485 mg/mL. The DPPH radical, a stable free radical compound, is widely employed to evaluate the radical scavenging activity of nanoparticles due to its sensitivity and simplicity.

Notably, at 0.91 mg/mL, AgNPs and 2.677 mg/mL, AuNPs demonstrate greater antioxidant activity of 89.24% and 70.46%, respectively. Standard Trolox, on the other hand, showed 91.19% inhibition at 0.012 mg/mL. The IC_{50} value of green-synthesized AgNPs, AuNPs and the trolox (standard) were 1.151, 1.485, and 0.006, respectively (Table 1). The results clearly demonstrate that Trolox exhibits remarkably high antioxidant activity even at very low concentrations. This reflects the high potency of Trolox as a pure antioxidant compound (91.19% inhibition at 0.012 mg/mL; $IC_{50} = 0.006$). In contrast, AgNPs and AuNPs show slightly lower antioxidant activity even at higher concentrations compared to Trolox. However, AgNPs, in particular, exhibited a relatively high inhibition rate of 89.24% at 0.91 mg/mL and showed a more effective profile than AuNPs with an IC_{50} value of 1.151. AuNPs, on the other hand, demonstrated 70.46% inhibition at a higher concentration of 2.677 mg/mL, with an IC_{50} value of 1.485, indicating that their antioxidant activity is lower compared to AgNPs. The higher antioxidant activity of AgNPs is attributed to their surface chemistry and the coating structure formed with catechins and other phenolic compounds, which facilitate a more effective transfer of electrons or hydrogen atoms to DPPH radicals. These interactions result in the formation of more active sites on the surface of AgNPs, enabling enhanced neutralization of free radicals [65]. Furthermore, the smaller size and higher surface-to-volume ratio of AgNPs are additional factors that contribute to their antioxidant effect. This can be explained by the fact that catechins provide a more effective coating and stabilization while reducing silver ions [65, 66]. In conclusion, in our study, AgNPs exhibited higher antioxidant activity than AuNPs due to their high surface reactivity, more effective catechin coating, and the easier interaction of surface functional groups with radicals such as DPPH.

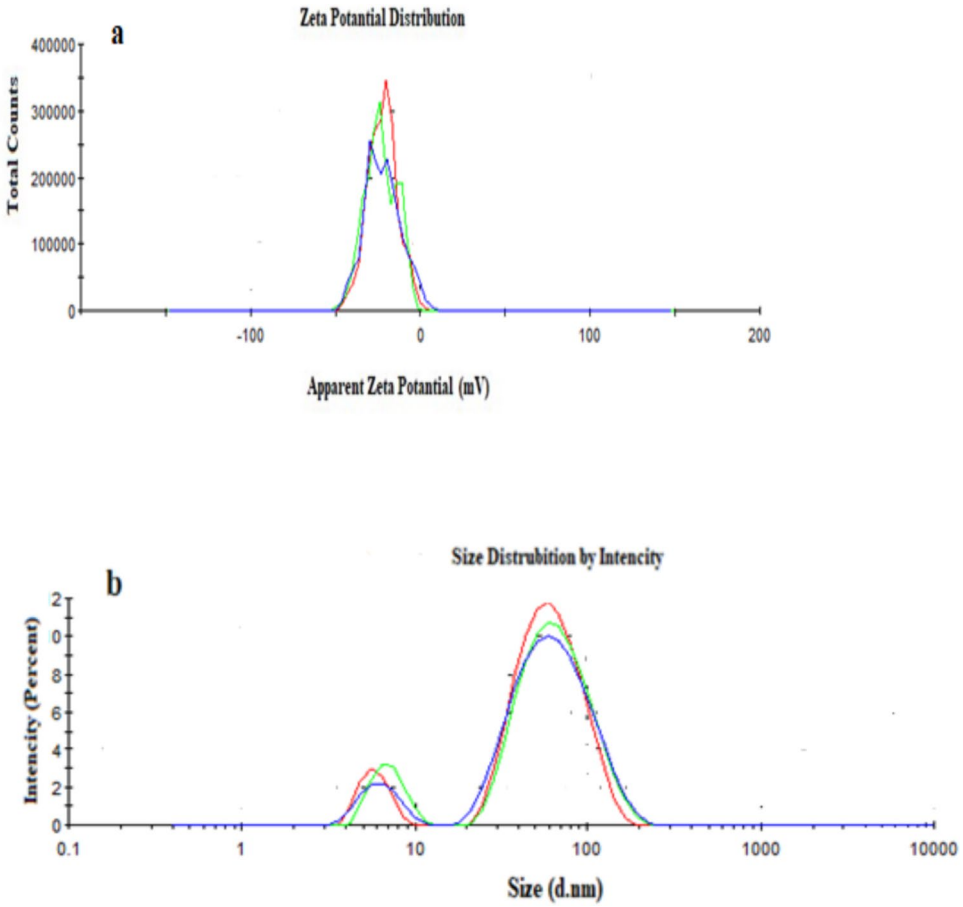

Fig. 15 **a** Zeta potential and **b** size distribution of Au nanoparticles synthesized with 0.5 mM $HAuCl_4.3H_2O$ and 0.5 mL catechin extract at 25 °C

Table 1 DPPH radical scavenging activity of biosynthesized silver nanoparticles (AgNPs), gold nanoparticles (AuNPs), and Trolox (standard)

Sample	Concentration in mg/mL	Scavenging activity in %	IC_{50} value in mg/mL
Biosynthesized silver nanoparticles (Ag-NPs)	0.113	21.70 ± 13.9	1.151 ± 0.29
	0.227	32.62 ± 30.5	
	0.455	57.50 ± 13.4	
	0.91	89.24 ± 7.05	
Biosynthesized gold nanoparticles (Au-NPs)	0.334	5.236 ± 3.64	1.485 ± 0.23
	0.669	19.00 ± 1.09	
	1.338	38.07 ± 3.28	
	2.677	70.46 ± 5.57	
Trolox (standard)	0.001	15.03 ± 5.45	0.006 ± 0.001
	0.003	42.46 ± 10.2	
	0.006	51.94 ± 9.10	
	0.012	91.19 ± 2.64	

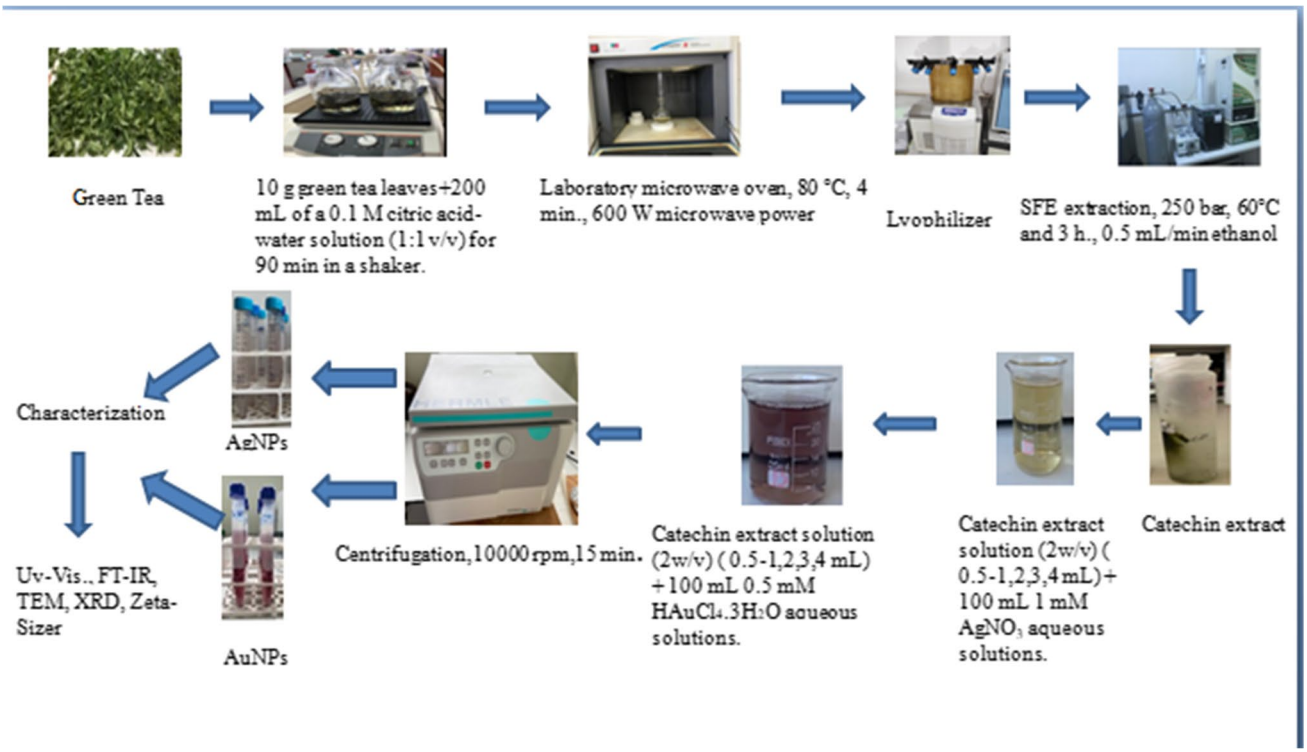

Fig. 16 IC_{50} values of the biosynthesized AgNPs, AuNPs, and Trolox

Discussion and Conclusion

The SPR absorption peaks presented in Figs. 2, 3, 4, 5, 6, and 7 were recorded at temperatures of 25, 35, and 45 °C using varying volumes (0.5–4 mL) of aqueous extract solutions under magnetic stirring. UV–Vis spectrophotometric analyses were conducted at time intervals ranging from 1 to 240 min for AgNPs and from 1 to 60 min for AuNPs. The effects of temperature and extract volume on the synthesis of AgNPs and AuNPs were evaluated. The most intense and narrow SPR absorption peaks for both nanoparticle types were observed at 25 °C. Among the tested synthesis temperatures (25 °C, 35 °C, and 45 °C), 25 °C was found to be the optimal condition for both AgNPs and AuNPs, as evidenced by the narrower and more intense SPR peaks observed at this temperature. Nanoparticle synthesis carried out at 25 °C proceeds through a kinetically controlled mechanism, contributing to the formation of smaller, more uniform, and more stable nanoparticles. This is evidenced by the narrow SPR peaks observed and ensures high performance and reliability in biomedical and optical applications. The

successful synthesis of AgNPs and AuNPs was confirmed by a comprehensive set of characterization techniques, including UV–Vis spectroscopy, TEM, DLS, FT-IR, and XRD. Although their antioxidant activity was slightly lower than that of the synthetic antioxidant Trolox, the green-synthesized AgNPs and AuNPs exhibited considerable free radical scavenging capacity, demonstrating their potential as effective antioxidant agents. Green-synthesized nanoparticles represent eco-friendly and sustainable alternatives to conventional antioxidants, offering considerable advantages due to their biocompatibility. In summary, this study successfully demonstrated the green synthesis of AgNPs and AuNPs using catechin extracts obtained through SFE at 25 °C. The results confirm that SFE-derived catechins function effectively as both reducing and stabilizing agents. Overall, the findings highlight the potential of this environmentally benign method for the sustainable production of metal nanoparticles with significant applicability in biomedical and pharmaceutical fields.

Acknowledgements The authors thank Karadeniz Technical University for its financial support (BAP03 Project No. FBB-2019-8049) and Karadeniz Technical University and Atatürk University's Central Research Laboratories.

Author Contribution Gönül SERDAR, Gülşah GÜL KILINÇ, Tuğba MAZLUM ŞEN: Investigation, Resources, Visualization, Formal Analysis, and Writing.

Funding Open access funding provided by the Scientific and Technological Research Council of Türkiye (TÜBİTAK). This research was funded by Karadeniz Technical University,Türkiye, Project No. BAP03 (FBB-2019–8049).

Data Availability No datasets were generated or analysed during the current study.

Declarations

Conflict of interest The authors declare no competing interests.

References

1. Amina SJ, Guo BA (2020) Review on the synthesis and functionalization of gold nanoparticles as a drug delivery vehicle. Int J Nanomedicine 15:9823–9857
2. Nirmal NP, Mereddy R, Li L, Sultanbawa Y (2018) Formulation, characterisation and antibacterial activity of lemon myrtle and anise myrtle essential oil in water nanoemulsion. Food Chem 254:1–7
3. Bergal A, Matar GH, Andaç M (2022) Olive and green tea leaf extracts mediated green synthesis of silver nanoparticles (AgNPs): comparison investigation on characterizations and antibacterial activity. BioNanoScience 123:07–321
4. Signati L, Allevi R, Piccotti F, Albasini S, Villani L, Sevieri M, Bonizzi A, Corsi F, Mazzucchelli S (2021) Ultrastructural analysis of breast cancer patient-derived organoids. Cancer Cell Int 21:423
5. Sevieri M, Silva F, Bonizzi A, Sitia L, Truffi M, Mazzucchelli S, Corsi F (2020) Indocyanine green nanoparticles: are they compelling for cancer treatment? Front Chem 8:535
6. Zhang Y, Li M, Gao X, Chen Y, Liu T (2019) Nanotechnology in cancer diagnosis: progress, challenges and opportunities. J Hematol Oncol 12(1):137
7. Ahmad M, Nirmal NP, Danish M, Chuprom J, Jafarzedeh S (2016) Characterisation of composite films fabricated from collagen/chitosan and collagen/soy protein isolate for food packaging applications. RSC Adv 6:82191–82204
8. Bharadwaj KK, Rabha B, Pati S, Sarkar T, Choudhury BK, Barman A, Bhattacharjya D, Srivastava A, Baishya D, Edinur HA et al (2021) Green synthesis of gold nanoparticles using plant extracts as beneficial prospect for cancer theranostics. Molecules 26:6389
9. Singla S, Jana A, Thakur R, Kumari C, Goyal S, Pradhan J (2022) Green synthesis of silver nanoparticles using Oxalis griffithii extract and assessing their antimicrobial activity. OpenNano 7:100047
10. Hassanisaadi M, Bonjar GH, Rahdar A, Pandey S, Hosseinipour A, Abdolshahi R (2021) Environmentally safe biosynthesis of gold nanoparticles using plant water extracts. Nanomaterials 11:2033
11. Perveen K, Husain FM, Qais FA, Khan A, Razak S, Afsar T, Alam P, Almajwal AM, Abulmeaty MMA (2021) Microwave-assisted rapid green synthesis of gold nanoparticles using seed extract of Trachyspermum ammi: ROS mediated biofilm inhibition and anticancer activity. Biomolecules 11:197
12. Rabha B, Bharadwaj KK, Boro N, Ghosh A, Gogoi SK, Varma RS, Baishya D (2021) Cheilocostus speciosus extract-assisted naringenin-encapsulated poly-ε-caprolactone nanoparticles: evaluation of anti-proliferative activities. Green Chem 23:7701–7711
13. Lateef A, Ojo SA, Elegbede JA (2016) The emerging roles of arthropods and their metabolites in the green synthesis of metallic nanoparticles. Nanotechnol Rev 5:601–622
14. Duan H, Wang D, Li Y (2015) Green chemistry for nanoparticle synthesis. Chem Soc Rev 44:5778–5792
15. Singh P, Kim YJ, Zhang D, Yang DC (2016) Biological synthesis of nanoparticles from plants and microorganisms. Trends Biotechnol 34:588–599
16. Rashid MMO, Ferdous J, Banik S, Islam MR, Uddin A, Robel FN (2016) Anthelmintic activity of silver-extract nanoparticles synthesized from the combination of silver nanoparticles and Momordica charantia fruit extract. BMC Complement Altern Med 16(1):1–6
17. Ahmed S, Ahmad M, Swami BL, Ikram S (2016) A review on plants extract mediated synthesis of silver nanoparticles for antimicrobial applications: a green expertise. J Adv Res 7:17–28
18. Ebrahiminezhad A, Zare-Hoseinabadi A, Sarmah AK, Taghizadeh S, Ghasemi Y, Berenjian A (2018) Plantmediated synthesis and applications of iron nanoparticles. Mol Biotechnol 60:154–168

19. Shafey AME (2020) Green synthesis of metal and metal oxide nanoparticles from plant leaf extracts and their applications: a review. Green Process Synth 9:304–339
20. El-Naggar NEA, Hussein MH, El-Sawah AA (2018) Phycobiliprotein-mediated synthesis of biogenic silver nanoparticles, characterization, in vitro and in vivo assessment of anticancer activities. Sci Rep 8:1–20
21. Castillo-henr L, Alfaro-aguilar K, Ugalde- Alvarez J, Vega-fern L, Montes G, Oca-v D, Vega-baudrit JR (2020) Green synthesis of gold and silver nanoparticles from plant extracts and their possible applications as antimicrobial agents in the agricultural area. Nanomaterials 10(9):1763
22. Rama P, Mariselvi P, Sundaram R, Muthu K (2023) Eco-friendly green synthesis of silver nanoparticles from Aegle marmelos leaf extract and their antimicrobial, antioxidant, anticancer and photocatalytic degradation activity. Heliyon 9(6):e16277
23. Thiruvengadam M, Rajakumar G, Chung IM (2018) Nanotechnology: current uses and future applications in the food industry. 3 Biotech 8:1–13
24. Mittal AK, Chisti Y, Banerjee UC (2013) Synthesis of metallic nanoparticles using plant extracts. Biotechnol Adv 31:346–356
25. Ebrahiminezhad A, Raee MJ, Manafi Z, Sotoodeh Jahromi A, Ghasemi Y (2016) Ancient and novel forms of silver in medicine and biomedicine. J Adv Med Sci Appl Techn 2:122–128
26. Chung IM, Park I, Seung-Hyun K, Thiruvengadam M, Rajakumar G (2016) Plant mediated synthesis of silver nanoparticles: their characteristic properties and therapeutic applications. Nanoscale Res Lett 11:1–14
27. Singh P, Pandit S, Garnæs J, Tunjic S, Mokkapati VRSS, Sultan A, Thygesen A, Mackevica A, Mateiu RV, Daugaard AE, Baun A, Mijakovic I (2018) Green synthesis of gold and silver nanoparticles from Cannabis sativa (industrial hemp) and their capacity for biofilm inhibition. Int J Nanomedicine 13:3571–3359
28. Jadoun S, Arif R, Jangid NK, Meena RK (2021) Green synthesis of nanoparticles using plant extracts: a review. Environ Chem Lett 19:355–374
29. Azizi S, Mohamad R, Abdul Rahim R, Mohammadinejad R, Bin Arif A (2017) Hydrogel beads bio-nanocomposite based on kappa-carrageenan and green synthesized silver nanoparticles for biomedical applications. Int J Biol Macromol 104:423–431
30. Lee KX, Shameli K, Yew YP, Teow SY, Jahangirian H, Rafiee-Moghaddam R, Webster TJ (2020) Recent developments in the facile bio-synthesis of gold nanoparticles (AuNPs) and their biomedical applications. Int J Nanomedicine 15:275–300
31. Al Saqr A, Khafagy ES, Alalaiwe A, Aldawsari MF, Alshahrani SM, Anwer MK, Khan S, Lila ASA, Arab HH, Hegazy WAH (2021) Synthesis of gold nanoparticles by using green machinery: characterization and in vitro toxicity. Nanomaterials 11:808
32. Arshad R, Barani M, Rahdar A, Sargazi S, Cucchiarini M, Pandey S, Kang M (2021) Multi functionalized nanomaterials and nanoparticles for diagnosis and treatment of retinoblastoma. Biosensors 11:97
33. Koushki K, Keshavarz Shahbaz S, Keshavarz M, Bezsonov EE, Sathyapalan T, Sahebkar A (2021) Gold nanoparticles: multifaceted roles in the management of autoimmune disorders. Biomolecules 11:1289
34. Piktel E, Suprewicz Ł, Depciuch J, Chmielewska S, Skłodowski K, Daniluk T, Król G, Kołat Brodecka P, Bijak P, Pajor-Świerzy A et al (2021) Varied-shaped gold nanoparticles with nanogram killing efficiency as potential antimicrobial surface coatings for the medical devices. Sci Rep 11:12546
35. Kajani AA, Bordbar AK, Zarkesh Esfahani SH, Razmjou A (2016) Gold nanoparticles as potent anticancer agent: green synthesis, characterization, and in vitro study. RSC Adv 6:63973–63983
36. Sharma N, Bhatt G, Kothiyal P (2015) Gold nanoparticles synthesis, properties, and forthcoming applications: a review. Indian J Pharm Biol Res 3:13–27
37. Shah M, Fawcett D, Sharma S, Tripathy SK, Poinern GEJ (2015) Green synthesis of metallic nanoparticles via biological entities. Materials 8:7278–7308
38. Mude N, Ingle A, Gade A, Rai M (2009) Synthesis of silver nanoparticles using callus extract of Carica papaya—a first report. J Plant Biochem Biotechnol 18:83–86
39. Koina IM, Sarigiannis Y, Hapesh E (2023) Green extraction techniques for the determination of active ingredients in tea: current state, challenges, and future perspectives. Separations 10(2):121
40. Kamal SSK, Sahoo PK, Vimala J, Premkumar M, Ram S, Durai L (2020) Novel green chemical route for synthesis of silver nanoparticles using Camellia sinensis. Acta Chim Slov 57:808–812
41. Flores-González M, Talavera-Rojas M, Soriano-Vargas E, Rodríguez-González V (2018) Practical mediated-assembly synthesis of silver nanowires using commercial Camellia sinensis extracts and their antibacterial properties. New J Chem 42:2133–2139
42. Seabra AB, Manosalva N, Lima BA, Pelegrino MT, Brocchi M, Rubilar O, Durán N (2017) Antibacterial activity of nitric oxide releasing silver nanoparticles. J Phys Conf Ser 838
43. Moulton MC, Braydich-Stolle LK, Nadagouda MN, Kunzelman S, Hussaina SM, Varma RS (2010) Synthesis, characterization and biocompatibility of "green" synthesized silver nanoparticles using tea polyphenols. Nanoscale 2:763–770
44. Flieger J, Franus W, Panek R, Szymańska-Chargot M, Flieger W, Flieger M, Kołodzie P (2021) Green synthesis of silver nanoparticles using natural extracts with proven antioxidant. Molecules 26:4986
45. Sökmen M, Alomar SY, Albay C, Serdar G (2017) Microwave assisted production of silver nanoparticles using green tea extracts. J Alloys Compd 725:190–198
46. Serdar G, Gül Kılınç G (2023) Microwave assisted production and characterization of gold nanoparticles using green tea and catechin extracts obtained by supercritical extraction method. Chem Pap 77:5155–5167
47. Serdar G (2015) Yaş çay ve siyah çay atıklarından mikrodalga yöntemi ile kafein ve kateşinlerin Yazım alanları gerektiği kadar uzatılabilir ekstraksiyonu. (Doktora Tezi), Karadeniz Teknik Üniversitesi Fen Bilimleri Enstitüsü
48. Demir E, Serdar G, Sökmen M (2015) Comparison of some extraction methods for isolation of Catechins and caffeine from Turkish green tea. Int J Secondary Met 2:16–25
49. Molyneux (2004) The use of the stable free radical diphenylpicrylhyrazyl (DPPH) for estimating antioxidant activity. Songklanakarin J Sci Technol 26:211–219
50. Serdar G (2023) Green biosynthesis of silver nanoparticles were obtained from the extract of pomegranate (Punica granatum L.) leaves by supercritical extraction using microwave method. Celal Bayar Üniversitesi Fen Bilimleri Dergisi 19:351–358
51. Serdar G (2021a) Biosynthesis of silver nanoparticles using extract of fig (Ficus carica) leaf by microwave extraction. Bull Biotechnol 2(2):44–50
52. Serdar G, Albay C, Sökmen M (2019) Biosynthesis and characterizatıon of silver nanopartıiles from the lemon leaves extract. Cumhur Scı J 40(1):170–172
53. Muthu K, Priya S (2017) Green synthesis, characterization and catalytic activity of silver nanoparticles using Cassia auriculata flower extract separated fraction. Spectrochim Acta A Mol Biomol Spectrosc 179:66–72
54. Serdar G (2024a) Gold nanoparticles biosynthesis through green synthesis mediated by leaf extract from Diospyros Kaki

L. (persimmon) using the microwave extraction method. Plasmonics 19:2813–2823
55. Serdar G (2024b) Biosynthesis and characterization of gold nanoparticles using microwave-assisted technology from pomegranate (*Punica granatum* L.) leaf extract produced by the method of supercritical fluid extraction (SFE). Plasmonics 19:2233–2243
56. Serdar G (2021b) Microwave-assisted green biosynthesis of gold nanoparticles from Eriobotrya Japonica leaf extract. Bull Biotechnol 2(2):38–43
57. Akilandaeaswari B, Muthu K (2020) Green method for synthesis and characterization of gold nanoparticles using Lawsonia inermis seed extract and their photocatalytic activity. Mater Lett 277:128344
58. Asghar MA, Zahir E, Shahid SM, Khan MN, Ashgar MA, Iqbal J, Walker G (2018) Iron, copper and silver nanoparticles: green synthesis using green and black tea leaves extracts and evaluation of antibacterial, antifungal and aflatoxin B1 adsorption activity. LWT - Food Sci Technol 90:98–107
59. Ghosh K, Satapathy SS, Ghosh S, Jauhari S, Kundu CN, Satyabrata S (2020) Green chemistry approach for gold nanoparticles synthesis using plant extracts: a potential material towards catalysis and biology. Adv Nat Sci : Nanosci Nanotechnol 11:035012
60. Geraldes AAS, Jessica L, Gethzemani MEV, Nilton L, Kattesh VK, Ademar BL, Adriana N (2016) Green nanotechnology from plant extracts: synthesis and characterization of gold nanoparticles. Adv Nanoparticles 5:176–185
61. Serdar G, Demir E, Bayrak S, Sökmen M (2016) New approaches for effective microwave assisted extraction of caffeine and Catechins from green tea. Int J Second Metab 3(1):3–13
62. Onitsuka S, Hamada T, Okamura H (2019) Preparation of antimicrobial gold and silver nanoparticles from tea leaf extracts. Colloids Surf B: Biointerfaces 173(1):242–248
63. Rolim WR, Pelegrino MT, de Araújo Lima B, Ferraz LS, Costa FN, Bernardes JS, Rodigues T, Brocchi M, Seabra AB (2019) Green tea extract mediated biogenic synthesis of silver nanoparticles: characterization, cytotoxicity evaluation and antibacterial activity. Appl Surf Sci 463:66–74
64. Jia JL, Xu HH, Li DQ, Ye WH, Liu WJ (2015) Biosynthesis of silver and gold nanoparticles using Huangdan (*Camellia sinensis*) leaf extract. Synthesis and Reactivity in Inorganic, Metal-Organic, and Nano-Metal Chemistry 45(7):941–946
65. Suresh P, Doss A, Praveen Pole RP, Devika M (2024) Green synthesis, characterization and antioxidant activity of bimetallic (Ag-ZnO) nanoparticles using *Capparis zeylanica* leaf extract. Biomass Convers Biorefinery 14:16451–16459
66. Iravani S (2011) Green synthesis of metal nanoparticles using plants. Green Chem 13(10):2638–2650